Optical Materials 110 (2020) 110458

Contents lists available at ScienceDirect

Optical Materials

journal homepage: http://www.elsevier.com/locate/optmat

Invited Article

Structural investigation and optical enhancement characterization of nanostructured Ga-doped @CdO/FTO films for photodiode applications

A.A.A. Farag [a,*], A.M. Aboraia [b,c], H. Elhosiny Ali [d,e], V. Ganesh [d], H.H. Hegazy [d], Alexander V. Soldatov [b], H.Y. Zahran [d,f], Yasmin Khairy [e], I.S. Yahia [d,f,g]

[a] Physics Department, Faculty of Education, Ain Shams University, Roxy, 11757, Cairo, Egypt
[b] The Smart Materials Research Institute, Southern Federal University, Sladkova, 178/24, 344090, Rostov-on-Don, Russia
[c] Department of Physics, Faculty of Science, Al-Azhar University, Assiut, 71542, Egypt
[d] Advanced Functional Materials & Optoelectronic Laboratory (AFMOL), Department of Physics, Faculty of Science, King Khalid University, 9004, Abha, Saudi Arabia
[e] Physics Department, Faculty of Science, Zagazig University, Zagazig, 44519, Egypt
[f] Nanoscience Laboratory for Environmental and Bio-medical Applications (NLEBA), Semiconductor Lab., Metallurgical Lab.1, Physics Department, Faculty of Education, Ain Shams University, Roxy, 11757, Cairo, Egypt
[g] Research Center for Advanced Materials Science (RCAMS), King Khalid University, Abha 61413, 9004, Saudi Arabia

ARTICLE INFO

Keywords:
Thin film
Kramer-kronig approach
Energy gap
Dispersion parameters

ABSTRACT

In this work, the high quality of CdO film with a different percentage of Ga doping prepared onto optically flat glass substrates using a sol-gel spin coating progression for enhancement of its structural characteristics for various applications. X-ray diffraction results confirm that the prepared films of CdO are amorphous due to the long-range array of deposited crystals. The images of the atomic force microscopy indicated that the surface morphology of the pure and Ga-doped CdO films has high roughness values of 60–80 nm and average particle size 85–100 nm. The optical constants were calculated using the Kramer-Kronig approach. The calculated optical transmission specifies a high transmission exceeding from 77% to 85% through the non-absorbing region depending on the doping concentrations. The results confirm that the measured optical band gap is strongly influenced by doping concentrations of Ga and decreases from 2.35 to 1.72 eV. The calculated optical dispersion and non-linear optical parameters were found to be strongly affected by doping. The terahertz cut-off frequency was set for the pure and Ga-doped CdO films indicating the applicability of the prepared films as terahertz filters.

1. Introduction

Cadmium oxide (CdO) thin films are one of the most widely promising compounds due to its unique properties and the presence of many applications and technological fields such as chemical sensors and battery production coloring dyes optical optoelectronic devices solar cells due to its semiconducting properties with high electron mobility, high electrical conductivity, chemical stability, and a direct bandgap (2.49 eV–2.51 eV) [1–4].

The CdO's doping with incorporating a suitable metal ion is a superior tool and may alter and improve its structural, optical, and electrical properties for various applications [5].

Turgut and Tatar [6] have studied the properties of the structural, electrical properties of the sol-gel deposited Sc-doped CdO films. They found that the properties of CdO have greatly affected by the contribution of Sc-content. While Gupta et al. [7] have concluded that the highest photocatalytic activity was recorded for the 7.5% Zn–CdO due to the mutual consequence of improved e-h separation and lower bandgap energy compared to the undoped CdO. Sahin et al. [8] have synthesized Ba-doped CdO films by the SILAR technique and revealed that the determined CdO band gap was believed to contribute to various technological appliances. Gupta et al. [9] have recorded a red-shift for the absorption spectra of Cu-doped CdO when compared with pure CdO.

Films of CdO and its dopants were fabricated by numerous methods like spray pyrolysis, RF-sputtering, successive ionic layer adsorption and reaction, pulsed laser, thermal evaporation, chemical bath deposition, metal-organic chemical vapor deposition, and sol-gel spin coating [10–18]. The sol-gel spin coating, used in this study, is characterized by various advantages such as low cost, easy for controlling the chemical stoichiometry and the metal doping concentrations [15–18].

* Corresponding author. , .
E-mail addresses: alaafaragg@gmail.com, alaafaragg@edu.asu.edu.eg (A.A.A. Farag).

https://doi.org/10.1016/j.optmat.2020.110458
Received 16 August 2020; Received in revised form 19 September 2020; Accepted 21 September 2020
Available online 3 October 2020

To the best of our information, so far, few studies have been accomplished on Ga doped @ CdO for condensed structural ad optical investigations. One of the most important of the current works on the optical properties of CdO and its metal doping effect is still a major in-depth study from researchers to enhance the extracted optical parameters for various applications. With all the available information, interest, and discussion of optimizing the performance of CdO properties, our team wants to give more understanding of the structural and optical optimization using Ga dopants of CdO for the application of a multi-functional device. Consequently, the current work aims to investigate the effect of one of the important metal dopant, Ga, with different concentrations on the structural and optical characteristics of CdO for optoelectronic device applications. The films of different structures depending on the dopant concentration were prepared by a low-cost sol-gel spin coating with good controlled, and appropriate film thickness. The crystalline and morphological structure confirmation were achieved by X-ray diffraction, and AFM microscopy, respectively. The optical constants were calculated using the Kramer-Kronig approach followed by the investigation of the optical parameters and the optical energy gap of pure and Ga-doped CdO films. A significant comparative investigation of the results presented with those in the literature for a similar structure and the associated optoelectronic applications were offered.

2. Experimental

2.1. Nanostructured Ga-doped CdO thin film preparation

The utilized method for depositing Ga doped @ CdO thin films is the well-known spin coating with the help of sol-gel on a clean glass substrate. The primary materials used are cadmium acetate, Cd $(CH_3COO)_2{\cdot}2H_2O$, and gallium nitrate, $Ga(NO_3)_3$ of high quality purchased from Sigma Aldrich with a molecular weight of 266.52 g/mol and 273.75 g/mol, respectively and using 2-Methaoxy ethanol as a solvent. Then the mixture was stirred continuously using a magnetic stirrer at a specific temperature of 60 °C to enable a homogeneous solution, after which MEA was added with stirring for an hour for obtaining a sol. Finally, the sol is reserved for approximately 48 h to obtain a gel formation, which the substrates are coated by using a spin coater operates at 1500 rpm for 50 s followed by a drying process for the layer at 120 °C to get rid of any excess of organic residue. For obtaining 1%, 5%, 7%, and 10% of Ga as dopant films, suitable amounts of Ga $(NO_3)_3$ were used.

2.2. Characterization techniques

The crystal structure of the films was investigated using the x-ray diffractometer type Shimadzu Lab X with CuK_α radiation. The Raman spectra of the films were recorded using TS, DXR FT-Raman spectrometer in the wavenumber range of 200–2000 cm^{-1}. The surface morphology of the Ga doped CdO films was investigated by using atomic force microscope (AFM), model NT-MDT. The optical properties of the prepared films were studied using a spectrophotometer JASCO UV-VIS-NIR 570.

2.3. Kramer-Kronig calculations for optical constants extraction

Several methods were used to calculate the optical constants of the material [19–22]. In comparison with these approaches, Kramer-Kronig relations can be considered more accurate. Moreover, the calculation of optical constants depends only on reflection data without the need for detailed information on any boundary conditions as well as does not depend on the measurement of the thickness of the samples, which greatly affects the calculations of optical constants. In this work, Kramer-Kronig relationships were employed to exactly analyze the optical constants of the studied films.

According to the Kramers-Kronig approach, the optical constants of n (ω) and k (ω). can be obtained using $N^{'}$ as follows [19–22]:

$$N^{'}(\omega) = n(\omega) + ik(\omega), \tag{1}$$

where

$$n(\omega) = \frac{1 - R(\omega)}{1 + R(\omega) - 2\sqrt{R(\omega)}cos\varphi(\omega)}, \tag{2}$$

and

$$k(\omega) = \frac{2\sqrt{R(\omega)}sin\varphi(\omega)}{1 + R(\omega) - 2\sqrt{R(\omega)}cos\varphi(\omega)}, \tag{3}$$

where φ (ω) is the phase difference, derived from the Fourier transform of *K–K* dispersion relation as follows:

$$\phi(\omega) = -\left(\frac{\omega}{\pi}\right)\int_0^\infty \frac{lnR(\omega^{'}) - lnR(\omega)}{\omega^{'2} - \omega^2}d\omega^{'}, \tag{4}$$

The Fourier transform of Eq. (3) is as follow:

$$\phi(\omega_i) = \frac{4\omega_i}{\pi} \times \Delta\omega_i \times \sum_i \frac{ln\sqrt{R(\omega)}}{\omega_i^{'2} - \omega_j^{'2}}, \tag{5}$$

where

$$\Delta\omega_j = \omega_{j+1} - \omega_j, \tag{6}$$

Where i = 2,4,6, …, j-1, j + 1, …for odd j and i = 1,3,5, …, j-1, j + 1, …for even j.

3. Results and discussion

3.1. Crystalline and morphological structure of pure and Ga-doped CdO thin films

The structural investigation of CdO and Ga-doped CdO films was performed using an X-ray diffraction pattern and shown in Fig. 1. There are no distinct peaks of the pure CdO thin film due to the amorphous nature. While the preferred orientation peaks are recorded at 32.96°, 38.18° with the corresponding Millar indices of (111) and (200), respectively of the Ga-doped CdO. The results are in agreement with the cubic phase of CdO and the JCPDS Card No.: 05–0640 and the lattice constant, a, is calculated and found to be 4.70 Å. The preferred diffraction peaks of the Ga-doped @CdO display a slight shift when compared with the influence of doping concentration. This small change

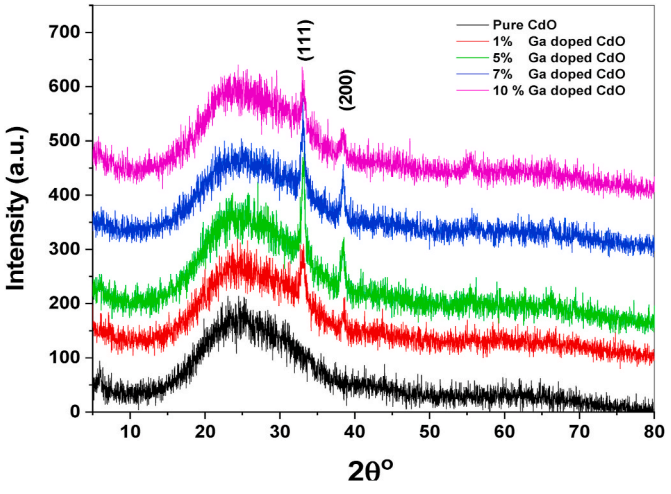

Fig. 1. XRD pattern of pure CdO and % Ga doping content @ CdO film.

can be attributed to the incorporation of Ga ions occupying Cd sites that affect the structural microstrain and the stoichiometry. These results are in agreement with those published by Thambidurai et al. [22], Şahin [23], and Gürbüz et al. [24].

Moreover, the intensity and the full width at half maxima (FWHM) intensity of diffracted peaks, differ for the concentration of Ga-doped @ CdO films, indicating differences in crystalline size and the microstrain and consequently the related parameters.

The mean crystalline size, D can be extracted from the results of XED using the FWHM of each peak, β using the following Scherrer's formula [26]:

$$D = \frac{K\lambda}{\beta \cos\theta} \tag{7}$$

The value of D of the Ga-doped CdO films as well as the FWHM were calculated for the (111) peak and plotted as a function of Ga-doping concentration as shown in Fig. 2(a) and listed in Table 1. The results indicate that the Ga-doping change the FWHM as well as the mean crystallite size of the films and agree with the results obtained by Gürbüz et al. [25]. The variation in crystalline size is due to the deviation of the CdO host lattice by adding Ga-dopants that influences the rate of CdO growth [27].

The properties of film microstrain, ε and the related dislocation,δ affect the main properties of the Ga-doped CdO and can be calculated by the following [25]:

$$\varepsilon = \frac{\beta \cos\theta}{4} \tag{8}$$

and

$$\delta = \frac{15\varepsilon}{aD} \tag{9}$$

The extracted values of δ and ε are listed in Table 1, and plotted as a function of Ga-dopant concentration (Figs. 2(b) and Fig.3(a, b)). Also, the relative intensity of the preferred orientations of the planes (111)/(200) is also represented in Fig. 2(b). As observed, opposite relationships between the crystalline size and the dislocation density. Moreover, similar results were recorded in the literature by Kumarn et al. [28] and Şahin [24].

3.2. Raman spectra of pure and Ga-doped @CdO thin films

Fig. 4 shows the Raman spectra of the pure and Ga doped CdO films. The figure shows a broad peak at ~290 cm^{-1} for the pure CdO. This broad peak is in agreement with those results obtained by Güney and İskenderoğlu [29]. This peak is related to the mixture of the influence of transverse sound and optical phonon which can be explained as a lattice disturbance of CdO. Moreover, the peaks centered around ~557 cm^{-1} are particularly detected for the Ga-doped CdO and can be associated with the crossing of the band through the transverse optical modes and the longitudinal optical vibration of the film and in agreement with those published in the literature [30,31]. The other detected peaks centered at ~1100 cm^{-1} of the pure and Ga-doped CdO films can be seen particularly Zn doped CdO can be associated with the longitudinal optical modes as discussed by Jambure, and Lokhande [32]. Table 2 lists the detected peaks of pure and Ga-doped CdO, in comparison with those published in the literature [33–35]. The most results of the experimental and theoretical of Raman spectroscopy done by various authors such as Bilz et al. [36], Popovic et al. [37], Ashrafi et al. [38], and Cusco et al. [39], have been attributed to the well-known modes to the transverse and longitudinal of CdO with a probable internal compressing stress which might induce an additional surface influence.

3.3. Surface topography of pure and Ga-doped @CdO thin films

The surface morphology investigations of the films are important because it strongly influences the optical properties and performance of the optoelectronic cells [40]. The morphology of the prepared pure and Ga-doped CdO films was checked using the 2D and 3D images of AFM and shown in Fig. 5. The nanoparticle with semi-spherical grains can be detected on the surfaces of the prepared films. The distribution of the grains is nearly homogeneous and the fluctuations from the homogeneity are observed with the increasing the Ga-concentration content. Similar CdO nanostructures have been identified in previous studies [41–44]. The calculations of the RMS roughness analysis for a pure CdO and Ga-CdO are also shown in Fig. 5. The recorded values of RMS are variables depending on the structure and changing from region to another. This roughness evaluation has an essential influence on the quality of the prepared device for the optoelectronic [22].

3.4. Optical descriptions of Ga-doped @ CdO films

Thin-film optical characterizations can control reflection, refraction and transmit the specified wavelength of electromagnetic radiation and have many applications such as optoelectronic device cells, attenuator, and optical filters, etc., in the desired spectrum of electromagnetic radiation. Depending on the desired performance for the designing and applications, it is essential to firmly control the basic parameters of the film such as the film thickness, the film uniformity, and roughness as well as the film composition and stoichiometry [45].

The spectral measurements of transmittance T(λ) and reflectance R (λ) in a varied range of wavelength spectrum $300 \leq \lambda \leq 1000$ nm of pure and Ga-doped CdO thin films are shown in Fig. 6(a and b). As observed, the values of T% in the starting wavelength range of 300–400 nm increases sharply and shows a transmission edge. After this, the transmittance approaches its maximum value (73–82%) in the wavelength range of 700–1000 nm. Besides, the behavior of R % shows a remarkable peak that changes in its position with the Ga-CdO concentrations [24].

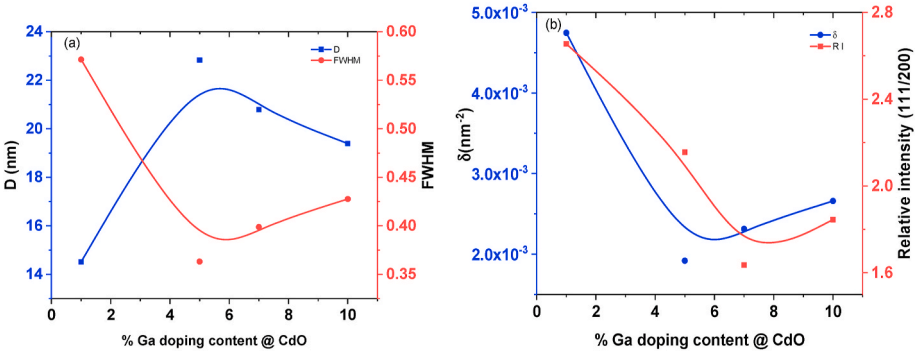

Fig. 2. Plot of (a) D and FWHM vs. % Ga doping content and (b) Plot of δ and relative intensity (111/200) vs. % Ga doping content of % Ga doping content @ CdO film.

Table 1
The calculated structural parameters of Ga-doped CdO/FTO films with different concentrations.

Structure	Diffraction plan	*D*(nm)	*ε*	*δ* (nm^{-2})	References
Pure	111	–	–	–	–
1%	111	14.51460874	0.002388	0.004746673	Present work
5%	111	22.83076539	0.001518	0.001918488	Present work
7%	111	20.79422631	0.001667	0.002312674	Present work
10%	111	19.38992069	0.001788	0.002659794	Present work
Pure	200	-	-	-	-
1%	200	21.45892317	0.001615	0.002171622	Present work
5%	200	16.28004235	0.002129	0.003773019	Present work
7%	200	26.43422124	0.001311	0.00143109	Present work
10%	200	14.22562721	0.002437	0.004941481	Present work

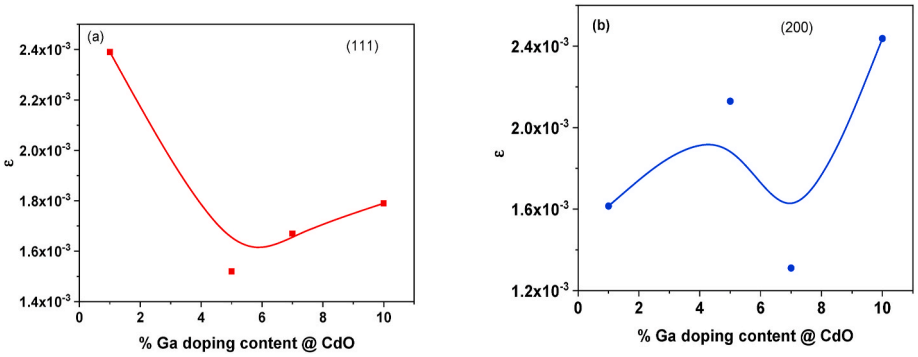

Fig. 3. Plot of (a) *ε* vs. % Ga doping content of (111) and (b) Plot of *ε* vs. % Ga doping content of % Ga doping content of (200) preferred orientation peak.

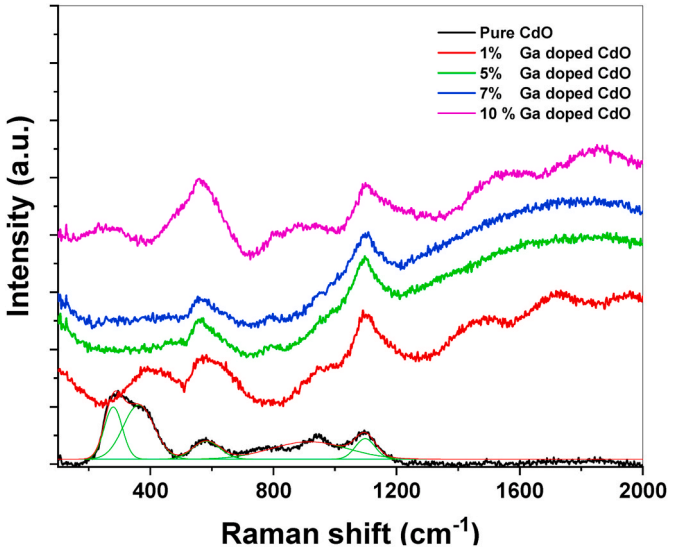

Fig. 4. Raman spectra of pure CdO and % Ga doping content @ CdO film.

Moreover, the dependency of R% on the Ga-dopant concentration changes is greater than those for T%. The recorded high values of *T(λ)*, as well as low values of *R(λ)*, enable the prepared films for optoelectronic devices application [46].

The behavior of the optical absorption spectra of the CdO and Ga-doped CdO films are shown in Fig. 7(a). The spectra show a blue shift compared to the pure CdO which can be due to the effect of the quantum restriction caused by the reduction of the particle size. The absorption spectra of Ga-doped CdO nanoparticles demonstrate that the edge of the absorption shifts slightly towards the longer wavelength when compared with the pure CdO nanoparticle. This shift specifies a decrease in the optical gap owing to the incorporation of the Ga-doping concentration. Fig. 7(b) shows the absorption spectra as a function of Ga-doped CdO at λ = 500 nm. This figure shows the change of the absorption spectra as the Ga-doping concentration change with a high value of the doping concentration of 7%.

Table 2
The Raman spectra maxima (cm^{-1}) of pure and Ga-doped CdO thin films.

Structure	Peak 1	Peak 2	Peak 3	Peak 4	References
Pure	291.6	571.4	941.8	1095.8	Present work
1%	409.2	585.3	–	1095.5	Present work
5%	–	562.7	–	1095.4	Present work
7%	–	566.9	–	1095.5	Present work
10%	–	566.99	–	1100.1	Present work
Pb-doped CdO	191, 269, 368	556	922	-	[33]
CdO	259.3329.9390.4	-	937.5	-	[34]
Zn-doped CdO	288	557	-	-	[35]

To obtain an accurate value of the energy gap of the CdO and Ga-doped CdO films, the analysis of the absorption coefficient, α nearby the edge of the energy range was utilized to obtain the optical gap, E_g according to the following relationship [21,22]:

$$\alpha = \frac{1}{d}\ln\left[\frac{(1-R)^2}{2T} + \sqrt{\left(\frac{(1-R)^4}{4T^2} + R^2\right)}\right]^{-1} \quad (10)$$

The relationship between the absorption coefficient and the energy gap can be expressed using the band theory as follows [21,22]:

$$\alpha h\nu = A\left(h\nu - E_g\right)^{1/2} \quad (11)$$

where *A* is a depending on the transition probability. The values E_g of the CdO and Ga-doped films were calculated using the plot of $(\alpha h\upsilon)^2$ vs. hυ of all the studied structures as shown in Fig. 8(a). The optical band gap, E_g values can be extracted from the intersects of the linear fitting part of the curve to satisfy the energy-axis. The extracted E_g values of the CdO

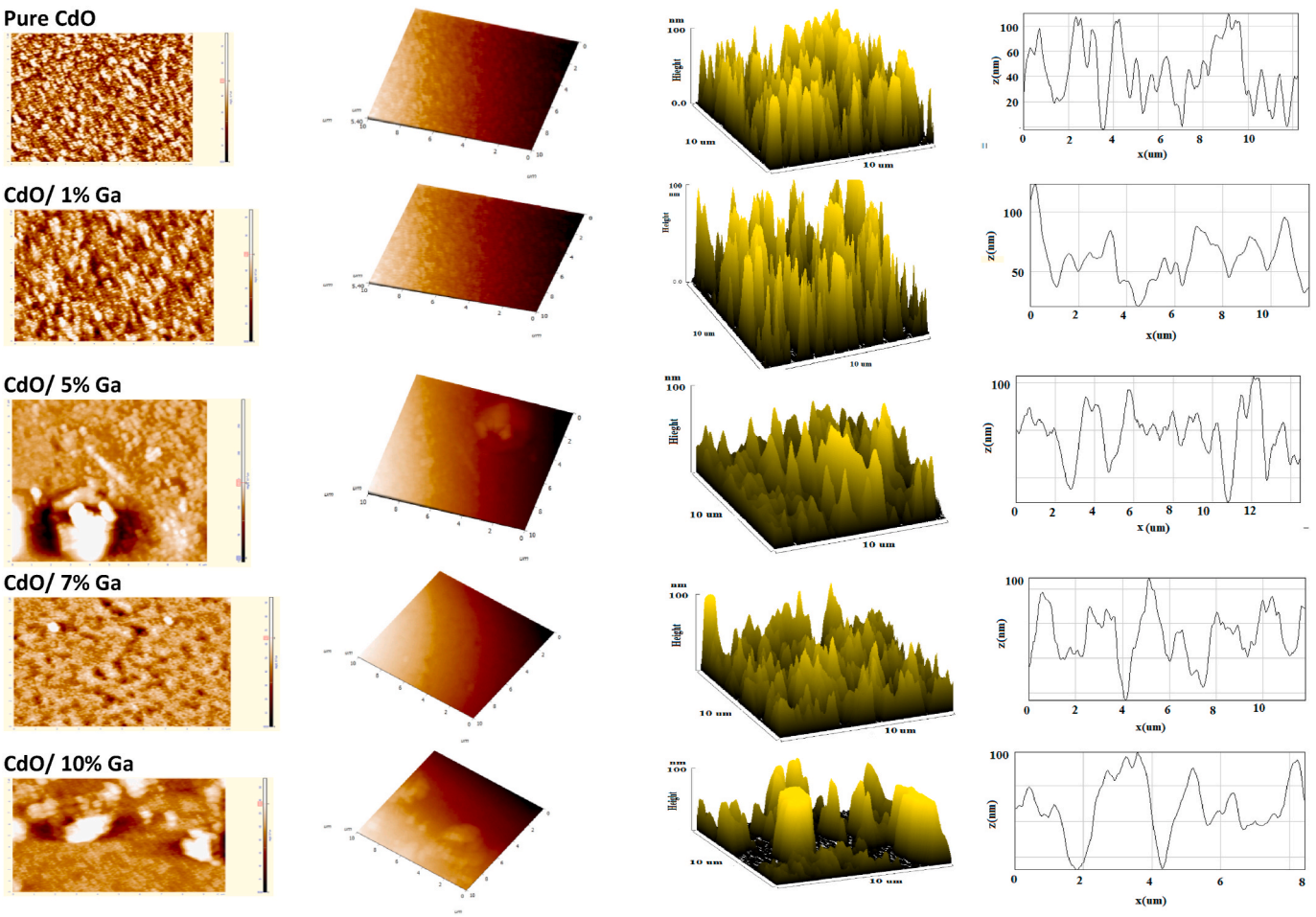

Fig. 5. 2-D and 3-D AFM images and roughness analysis of pure CdO and % Ga doping content @ CdO film.

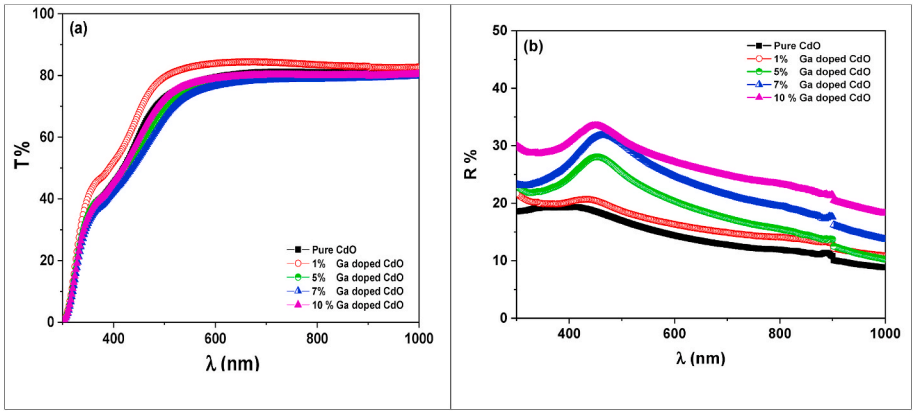

Fig. 6. The optical spectra of (a) transmittance, *T*, and (b) reflectance, *R*, versus wavelength of pure CdO and % Ga doping content @ CdO film.

and Ga-doped films are presented in Table 3 in comparison with those published in the literature for the related structures [2,47–49]. As observed from Fig. 8(b) and Table 3 that the values of E_g for CdO thin films reduced with increasing Ga-doping concentration which significantly improve the optoelectronic characteristics of CdO films. It is noted that there is an agreement in the behavior of decreasing the value of the energy gap by increasing the doping concentration as published in most of the literature. According to Alahmed et al. [50] for the Mn-doped CdO thin films, the calculated energy gaps were found to decrease from 2.41 eV to 1.7 eV for increasing the Mn doping concentration from 0 to 10%. While Dagdelen et al. [51] recorded a decrease of the energy gaps from 2.684 eV to 2.657 for the increase of the Bi-doping concentration to CdO. Yahia et al. [52] have studied the influence of Zn as a dopant for CdO and concluded that the energy gap reduced from 2.54 eV to 2.32 eV with increasing the Zn-doping concentration. Also, Yahia et al. [53] recorded the decrease of the energy gap of the Al-doped CdO from 2.54 to 2.32 eV when the doping concentration of the Al increases from 1% to 15%. Besides, Zhu et al. [54] have concluded that the energy gaps of In-doped CdO reduced from 3.1 eV to 2.4eV. The explanation for the reduction of the energy gap values

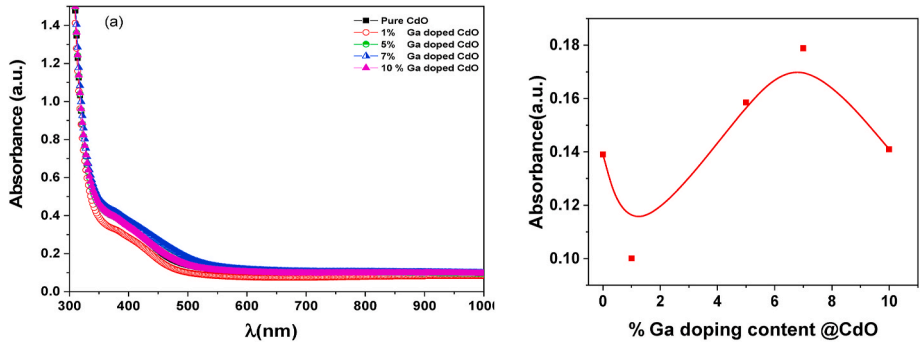

Fig. 7. Plot of (a) Absorption vs. λ and (b) Plot of Absorption vs. % Ga doping content of pure CdO and % Ga doping content @ CdO film.

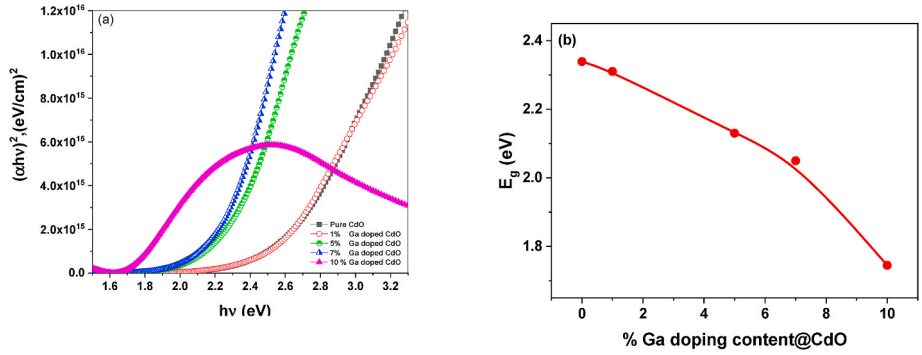

Fig. 8. Plot of (a) $(\alpha h\nu)^2$vs.hν and (b) Plot of E_g vs. % Ga doping content of pure CdO and % Ga doping content @ CdO film.

Table 3
The calculated energy gap and Urbach's energy of Ga-doped CdO/FTO films with different concentrations.

Structure	E_g (eV)	$E_{u,}$ (meV)	References
Pure	2.34	590	Present work
1%	2.31	372	Present work
5%	2.13	440	Present work
7%	2.05	427	Present work
10%	1.74	435	Present work
CdO/SLG	2.51	287	[2]
CdO/glass	2.64	392	[47]
CdO/glass	2.51	407	[48]
CdO/FTO	2.54	310	[49]

that are related to the incorporation of doping to CdO based on the structure modification of CdO thin films due to the deformation of the CdO structure due to either interstitial or interstitial Cd ions in the lattice of CdO by dopant [50]. This dopant like Ga ions will offer some additional energy levels into the CdO band gap near the valence band edge, and consequently, a reduction in the energy gap can be taken place.

Moreover, the absorption spectra of CdO and Ga-doped CdO show a specific shoulder at higher wavelengths associated with the absorption tail, called the Urbach tail [29]. This absorption can be analyzed to extract the Urbach energy, E_u using the following Eq [55].:

$$\alpha = \alpha_0 \left(\frac{h\nu}{E_u}\right) \tag{12}$$

The semilogarithmic plot of α *vs.* the photon energy of CdO and Ga-doped CdO is shown in Fig. 9(a). Using the best linear fit of the curves, shown in Fig. 9(a) for all the studied concentration, the values of E_u can be extracted and plotted as a function of Ga-doping concentration as shown in Fig. 9 (b) and collected in Table 3 in comparison with those value obtained for the similar CdO-dopant based structures [2,47–49]. As can be seen from the obtained values, the value of E_u influenced by the Ga-doping concentration and decrease with increasing its concentration. The shift of the Urbach's tail is expected to lead to a decrease in E_g due to the probable transition from the band to the tail as well as the increase of the localized states through the bandgap of the material due

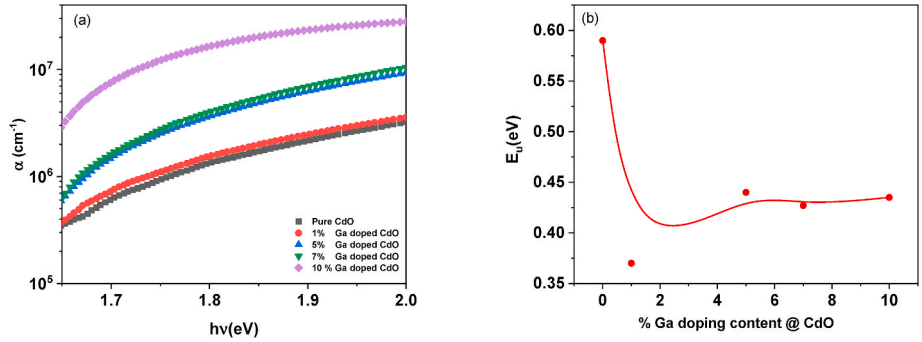

Fig. 9. Plot of (a) α vs. hν and (b) Plot of E_u vs. % Ga doping content of pure CdO and % Ga doping content @ CdO film.

to the incorporation of Ga atoms [23]. The recorded results are consistent with those published in the literature for similar related structures [2,47–49].

The main optical constants, namely, the extinction index, *k*, and the refractive index, *n* have been extracted using Kramer-Kronig relationships, detailed discussed above. The calculation of these parameters is significant for various designing of most optical components and related systems, especially for the optoelectronic devices. Because Kramers - Kronig investigation includes a wide-energy range integration, accordingly, the errors in any region might disturb the values derived in other energy ranges. The most important requirements for the best measurements with high accuracy are the smooth and cleaning of the sample surfaces which have been given the priority and significant attention in this study [56,57].

Fig. 10(a) shows that the spectral behavior of n values of the Ga-doped CdO films with observing two unique regions of the normal and abnormal regions, depending on the wavelength region and influenced by Ga-doped CdO concentration. Moreover, the values of k, shown in Fig. 10(b) shows also change in its values depending on the spectral range and ga doping concentrations. At λ = 780 nm, all the values of k approaches zero for all the studied samples due to the non-absorbtivity characteristics at this point. To obtain the main dispersion parameters, the single oscillator model has been applied for the non-absorbing region via DiDomenico and Wemple relationship [58]:

$$\left(n^2-1\right)^{-1}=\frac{E_0}{E_d}-\frac{(h\nu)^2}{E_0E_d} \tag{13}$$

Where E_0 is the energy oscillation, and E_d is the dispersion energy of the material. Fig. 11 (a) shows the $(n^2-1)^{-1}$ *vs.* $(h\nu)^2$ in the desired energy range. The values of E_0 and E_d can be extracted from the slope and intercept of the linear fit of the curves. The calculated E_d and E_0 are shown in Fig. 12(a) and (b), respectively, and tabulated in Table 4 for the studied the pure CdO and Ga-doped @CdO films. As observed, the values of E_d and E_0 shows a nonsystematic behavior with a minimum value for the 5% of Ga-doped CdO films. At this concentration, the value of energy gap is consistent with the oscillator energy, confirming the Eo/Eg ≈ 1, in agreement with those previously published by Elkanzi et al. [57] for organic films, Ravindra et al. [59] for various crystalline structure films, Tanaka [60] for some amorphous films.

Moreover, according to the DiDomenico and Wemple relationships, the E_0, E_d has a relation with the moments of dielectric constant, represented as M_{-1} and M_{-3} as follows [58]:

$$M_{-1}=\frac{E_d}{E_0} \tag{14}$$

and

$$M_{-3}=\frac{M_{-1}}{E_0^2} \tag{15}$$

The calculated values of both M_{-1} and M_{-3} plotted as a function of Ga-doped CdO of different concentrations, of the 7% Ga-doping concentration as compared to other concentrations, listed in Table 4 and shown in Fig. 13(a) and (b), respectively. The maximum values of both M_{-1} and M_{-3} are found to be for the Ga-dopant CdO of 7% concentration.

The other important parameter is the high-frequency dielectric constant, ε_∞ which can be calculated using the following [57]:

$$n^2=\varepsilon_\infty-\frac{1}{4\pi\varepsilon_0}\left(\frac{e^2}{c^2}\right)\left(\frac{N}{m^*}\right)\lambda^2 \tag{16}$$

The graphical representation n^2 vs. λ^2 is shown in Fig. 11 (b) for the pure CdO and Ga-doped CdO films. The values of ε_∞ and N/m^* can be extracted from the y-axis intersection and slope of the linear fit of the curves. The calculated ε_∞ and N/m^* are shown in Fig. 14(a) and (b), respectively, and tabulated in Table 4 for the studied the pure CdO and Ga-doped CdO films. These figures show increasing of both behavior of both ε_∞ and N/m^* with increasing the Ga-doping concentrations.

The real, ε_1, and imaginary, ε_2 dielectric constants can be calculated as follows [41]:

$$\varepsilon 1=n^2-k^2, and \varepsilon_2=2nk \tag{17}$$

The spectral dependence of ε_1 and ε_2 of the pure CdO and Ga-doped CdO films of various doping concentrations is shown in Fig. 15(a) and (b), respectively. The figures show that the values of ε_1 and ε_2 are strongly dependent on the doping concentration and the dependence systematically increases with increasing the doping concentration at λ = 750 nm and 650 nm for ε_1 and ε_2, respectively. Accordingly, the propagation of the electromagnetic waves is easy and fast through the films due to the low value of the dielectric constant as compared to the inorganic films [61].

The importance of optical conductivity, σ is due to the measurement of the conductivity of the material in the high ranges of applied frequencies that cannot be reached by the usual electrical measurements. Moreover, it is also characterized as a quantitative measurement free from direct contact with the sample as well as high sensitivity to charged response measurement. The two main components of σ_1 and σ_2 can be identified as in the literature [62,63] as follows:

$$\sigma_1=\omega\varepsilon_0\varepsilon_2 \tag{18-a}$$

$$\sigma_2=\omega\varepsilon_0\varepsilon_1 \tag{18-b}$$

The behavior of both σ_1 and σ_2 as a function of the wavelengths of the pure and Ga-doped CdO films is shown in Fig. 16(a) and (b). These figures illustrate distinctive optical conductivity peaks due to the characteristics of optical response and are affected by the Ga-doping concentration.

The study of nonlinear optics plays a major role in the basic applications of most optical devices such as optical signal processing units, optical computers, optical circuits, ultrafast switches, sensors, laser amplifiers, and laser amplifier devices [64].

The combination of the linear refractive index and the main parameters of the Wemple DiDomenico has been proposed by Ticha and

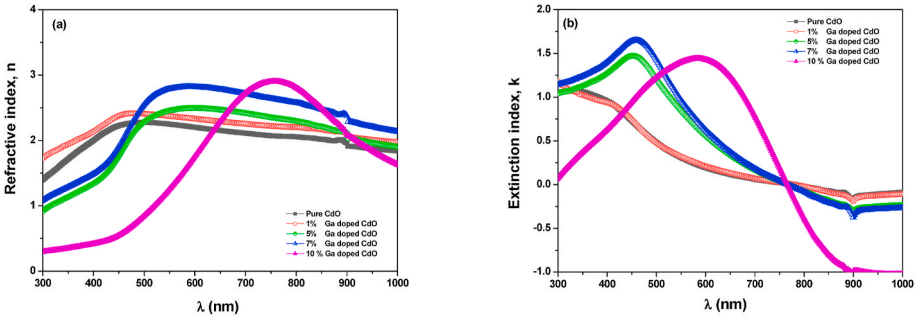

Fig. 10. The spectra of (a) refractive index, n, and (b) extinction index, k, vs. λ of pure CdO and % Ga doping content @ CdO film.

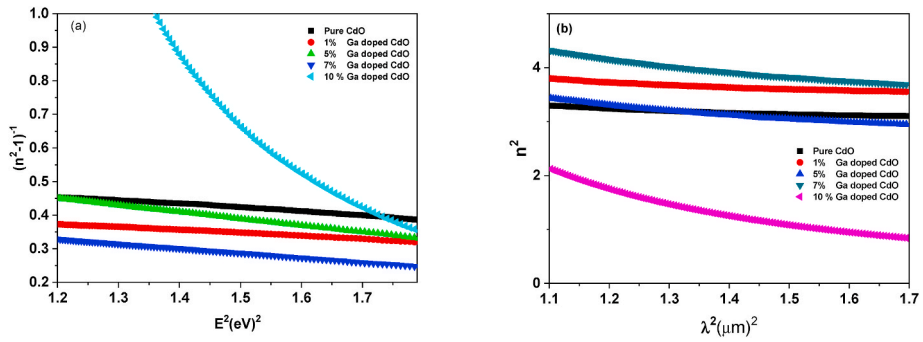

Fig. 11. Plot of (a) $(n^2\text{-}1)^{-1}$ vs. E^2 and (b) Plot of n^2 vs. λ^2 of Pure CdO and % Ga doping content @ CdO film.

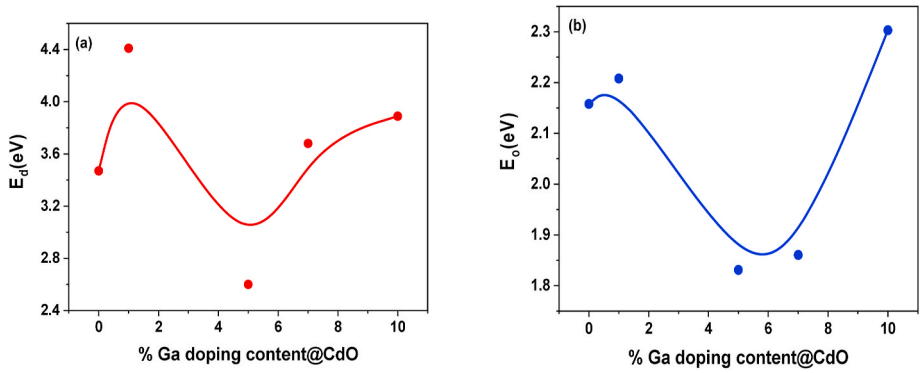

Fig. 12. Plot of (a) E_d vs. % Ga doping content and (b) Plot of E_0 vs. % Ga doping content of pure CdO and % Ga doping content @ CdO film.

Table 4
The calculated dispersion parameters of Ga-doped CdO/FTO films with different concentrations.

Structure	E_d(eV)	E_0(eV)	ε_∞	N/m*($10^{56}m^{-3}$/kg)	M_{-1} (eV)	M_{-3} $(eV)^{-2}$	References
Pure	3.45	2.15	3.69	4.41	0.55	0.34	Present work
1%	4.41	2.20	2.314	4.51	0.81	0.41	Present work
5%	2.56	1.82	2.134	9.97	0.598	0.42	Present work
7%	3.68	1.85	2.055	12.64	1.13	0.56	Present work
10%	2.89	2.29	1.745	34.19	0.53	0.32	Present work

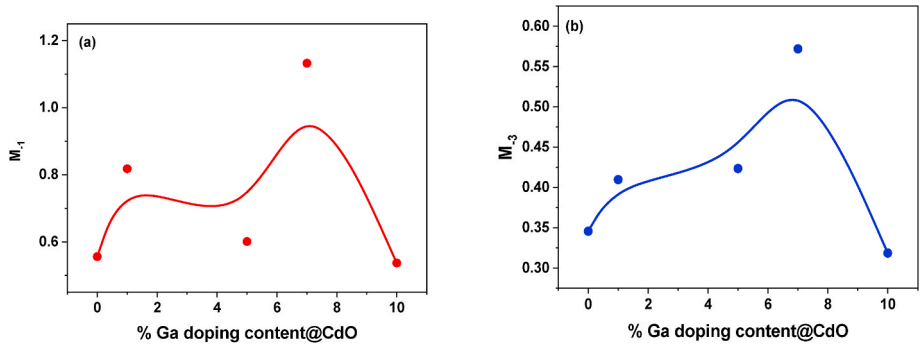

Fig. 13. Plot of (a) M_{-1} vs. % Ga doping content and (b) Plot of M_{-3} vs. % Ga doping content of pure CdO and % Ga doping content @ CdO film.

Tichy et al. [65] to extract the coefficient of the nonlinear polarization of the third-degree $\chi^{(3)}$ which can be determined as follows:

$$\chi^{(3)} = \frac{A}{(4\pi)^4}(n^2-1)^4 \tag{19}$$

where A is a constant, approximated for the most of materials and used for the Zn-doped CdO as 1.7×10^{-10} esu [65]. The nonlinear refractive index, $n^{(2)}$ is related to the static dielectric constant by the equation stated in the literature as follows [65,66].

$$n^{(2)} = \frac{12\pi\chi^{(3)}}{n_0} \tag{20}$$

The spectral dependence of the optical susceptibility, $\chi(1)$, 3rd order non-linear optical susceptibility, $\chi(3)$, and nonlinear refractive index, n (2) are shown respectively and shown in Fig. 17 and Fig. 18 for the pure and Ga-doped CdO films. These figures and Table 5 show a remarkable

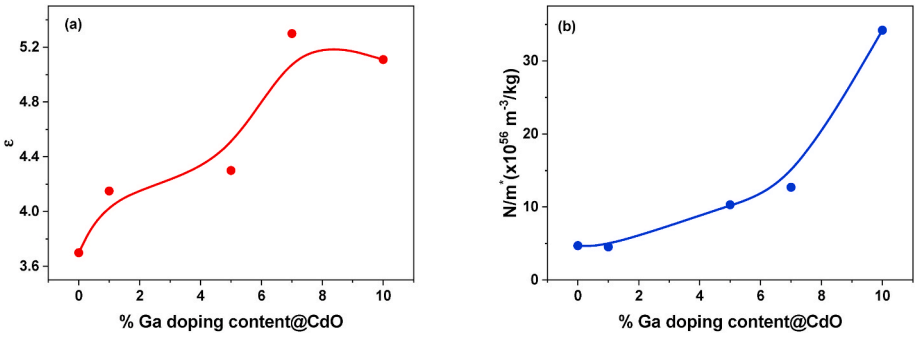

Fig. 14. Plot of (a) ε vs. % Ga doping content and (b) Plot of N/m*vs. % Ga doping content of pure CdO and % Ga doping content @ CdO film.

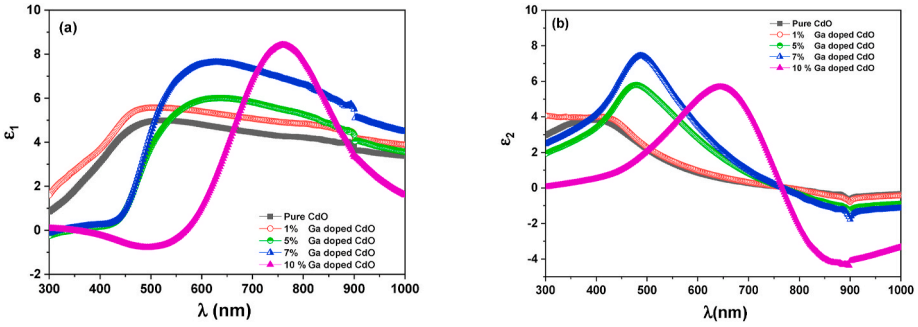

Fig. 15. The spectra of (a) real dielectric constant, ε_1, and (b) imaginary dielectric contant, ε_2 vs. λ of pure CdO and % Ga doping content @ CdO film.

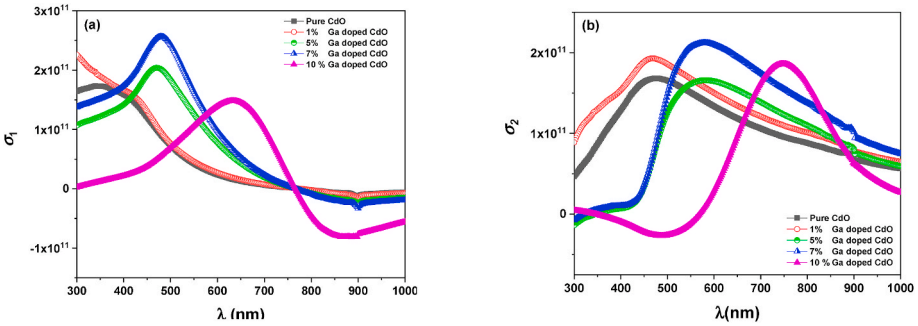

Fig. 16. The spectra of (a) real part of optical conductivity, σ $_1$, and (b) imaginary part of optical conductivity, σ_2, vs. λ of pure CdO and % Ga doping content @ CdO film.

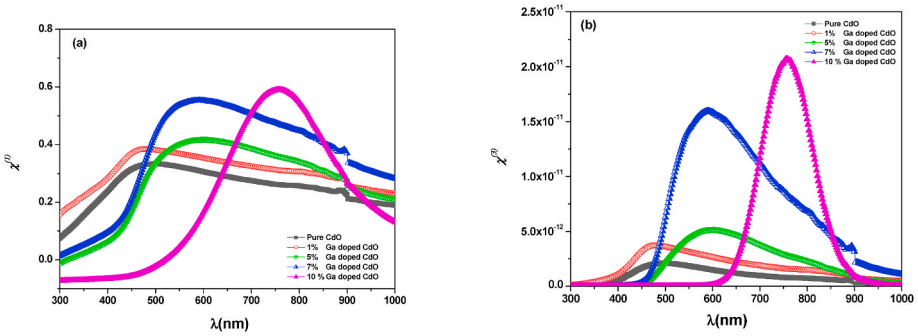

Fig. 17. The spectra of (a) $\chi^{(1)}$, and (b) $\chi^{(3)}$,vs. λ of pure CdO and % Ga doping content @ CdO film.

improvement of the nonlinear sensitivity as a result of Ga-incorporation of various concentrations in the lattice of CdO and affect the grain boundaries and change the amorphous state of CdO to nearly crystalline. Table 5 lists the results of $\chi(1)$, $\chi(3)$, and $n(2)$ in comparison with those published for similar structures [49,66]. The results show a good agreement with these published results. Typically, Ga incorporated in CdO contributes to the replacement of Cd^{2+} host ions with Ga^{2+} ions in the lattice of CdO. Accordingly, the films of Ga-doped CdO show an

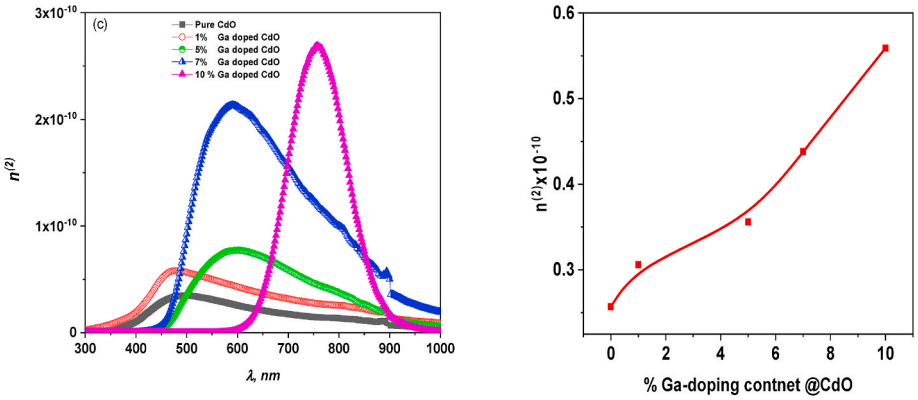

Fig. 18. Plot of (a) $n^{(2)}$ vs. λ and (b) Plot of $n^{(2)}$ vs. % Ga doping content of pure CdO and % Ga doping content @ CdO film.

Table 5
The calculated nonlinear parameters of Ga-doped CdO/FTO films with different concentrations.

Structure	$\chi^{(1)}$	$\chi^{(3)}$ (esu)	$n^{(2)}$ (esu)	References
Pure	1.3	5.7×10^{-13}	0.257×10^{-10}	Present work
1%	2.56	1.4×10^{-12}	0.306×10^{-10}	Present work
5%	3.68	2.4×10^{-12}	0.356×10^{-10}	Present work
7%	1.07	6.8×10^{-12}	0.438×10^{-10}	Present work
10%	2.7	1.4×10^{-11}	0.559×10^{-10}	Present work
Zn-doped CdO	0.13	5.73×10^{-14}	1.32×10^{-12}	[49]
Pure CdO	0.60	1.01×10^{-8}	2.80×10^{-12}	[66]
N doped CdO	1.62	1.24×10^{-9}	1.31×10^{-13}	[66]

improvement for both linear and non-linear optical characteristics and establish these structures for various future optoelectronic device applications.

3.5. The terahertz cut-off frequency of CdO films

Fig. 19(a–f) shows the influence of the Ga-doping concentration of CdO on terahertz cut-off frequency spectra. From the figure, it is evident that Ga-doping for CdO has a significant effect on the terahertz cut-off values. From the figure, it is evident that Ga-doping for CdO has a significant effect on the terahertz cut-off values. It is also evident from the figure that the increase of the Ga-doping concentration by 7% significantly increased the terahertz cut-off frequency values to 2.86 THz at 3.89 eV (Fig. 19d). The higher terahertz cut-off frequency of the 7% Ga-doping concentration of CdO film can be attributed to the lower value of the microstrain and the maximum absorption characteristic as compared to the other concentration. Moreover, a triple terahertz cut-off frequency is detected for the Ga-doping concentration by 10% (see Fig. 19e). Qasrawi and Alsabe [67] have reported that the higher the terahertz cut-off frequency, the more suitable of the material for the application of light communication performance. The determined terahertz cut-off frequency values specify that the pure CdO and Ga-doped CdO films of various doping concentrations can be used as active media for fabricating MOSFETs that are used for short-power analog and/or RF employment [68]. The increase in the terahertz cut-off frequency can be attributed to the lowering of the energy bandgap values due to the influence of the Ga-doping concentration of CdO. The terahertz cut-off frequency of the studied films is observed well as compared with those published by Alharbi and Qasrawi [69] for CdO films of various structures.

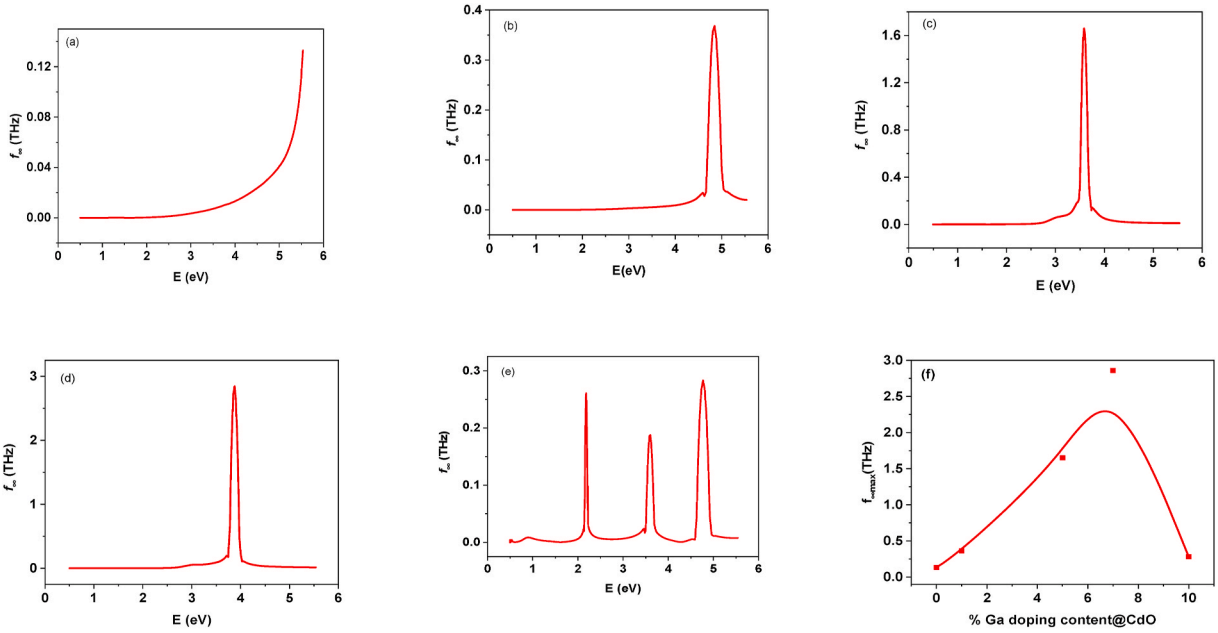

Fig. 19. Plot of f_{∞} vs. E of (a) pure CdO, (b) 1% Ga-doped, (c) 5% Ga-doped, (d) 7% Ga-doped, (e) 10% Ga-doped, and (f) Plot of $f_{\infty\ max}$ vs. % Ga doping content of pure CdO and % Ga doping content @ CdO film.

4. Conclusion

Thin films of CdO with various doping concentrations of Ga% were prepared by the sol-gel spin-coating technique and established by XRD and AFM images. The energy gaps were extracted from the analysis of the absorption coefficient at the absorption band edge and found to be direct and their values decreased from 2.35 to 1.72 eV depending on the doping concentration. The dispersion properties of the studied films were examined based on a single oscillator model using the Wemple-DiDomenico relationship, and the main parameters that confirmed the potential applications for optoelectronic devices were extracted. The oscillating energy of the films reached its lowest value ($E_0 = 1.84$ eV) as well as the oscillating energy ($E_d = 3.5$ eV) for the films of dopant concentration of 5%. The nonlinear optical parameters were examined to motivate enhancing the characteristics of the studied structures for the application of photodiode-based devices. The calculated values of terahertz cut-off frequency of the pure CdO and Ga-doped CdO films of various doping concentrations indicate the capability to usage these structures as active media for fabricating MOSFETs that are used for low-power applications.

CRediT authorship contribution statement

A.A.A. Farag: Writing - original draft, Formal analysis, Writing - review & editing. **A.M. Aboraia:** Methodology, Investigation. **H. Elhosiny Ali:** Writing - review & editing. **V. Ganesh:** Writing - review & editing. **H.H. Hegazy:** Methodology, Writing - review & editing. **Alexander V. Soldatov:** Methodology, Writing - review & editing. **H.Y. Zahran:** Methodology, Writing - review & editing. **Yasmin Khairy:** Methodology, Investigation, Formal analysis. **I.S. Yahia:** Conceptualization, Data curation.

Declaration of competing interest

The authors declare that they have no known competing financial interests or personal relationships that could have appeared to influence the work reported in this paper.

Acknowledgment

The authors express their appreciation to the Deanship of Scientific Research at King Khalid University for funding this work through research groups program under grant number R.G.P. 2/50/40.

References

[1] P. Velusamy, Ruimin Xing, R. Ramesh Babu, E. Elangovan, J. Viegas ShanhuLiu, M. Sridharan, A study on formaldehyde gas sensing and optoelectronic properties of Bi-doped CdO thin films deposited by an economic solution process, Sensor. Actuator. B Chem. 297 (2019) 126718.
[2] Murat Soylu, Solution molarity dependent structural and optical properties of CdO nanostructured thin films, Optik 216 (2020) 164865.
[3] Taj Muhammad Khan, Tauseef Shahid, M. Zakria, Rana I. Shakoor, Optoelectronic properties and temperature-dependent mechanisms of composite-hydroxide-mediated approach for the synthesis of CdO nanomaterials, Electron. Mater. Lett. 11 (2015) 366–373.
[4] M. Muraleedharan, H. Singh, S. Suresh, M. Udayakumar, Directly absorbing Therminol-Al_2O_3 nano heat transfer fluid for linear solar concentrating collectors, Sol. Energy 137 (2016) 134–142.
[5] A. Fakhri, S. Behrouz, M. Pourmand, Synthesis, photocatalytic and antimicrobial properties of SnO_2, SnS_2, and SnO_2/SnS_2nanostructure, J. Photochem. Photobiol., B 149 (2015) 45–50.
[6] G. Turgut, D. Tatar, Investigation of physical, electrical and optical properties of sol-gel deposited Sc-loaded CdO film, Optik 145 (2017) 292–303.
[7] V.K. Gupta, Ali Fakhri, S. Tahami, S. Agarwal, Zn doped CdO nanoparticles: Structural, morphological, optical, photocatalytic and anti-bacterial properties, J. Colloid Interface Sci. 504 (2017) 164–170.
[8] B. Sahin, Y. Gulen, F. Bayansal, H.A. Cetinkara, H.S. Guder, Structural and optical properties of Ba-doped CdO films prepared by SILAR method, Superlattice. Microst. 65 (2014) 56–63.
[9] R.K. Gupta, F. Yakuphanoglu, F.M. Amanullah, Bandgap engineering of nanostructure Cu doped CdO films, Physica E 43 (2011) 1666–1668.
[10] M. Zaien, N.M. Ahmed, Z. Hassan, Effects of annealing on the optical and electrical properties of CdO thin films prepared by thermal evaporation Mater, Lettres 105 (2013) 84–86.
[11] D.A. Lamb, S.J.C. Irvine, A temperature dependant crystal orientation transition of cadmium oxide films deposited by metal-organic chemical vapour deposition, J. Cryst. Growth 332 (2011) 17–20.
[12] B.J. Zheng, J.S. Lian, L. Zhao, Q. Jiang, Optical and electrical properties of Sn-doped CdO thin films obtained by pulsed laser deposition, Vacuum 85 (2011) 861–865.
[13] B. Saha, R. Thapa, K.K. Chattopadhyay, Bandgap widening in highly conducting CdO thin film by Ti incorporation through radio frequency magnetron sputtering technique, Solid State Commun. 145 (2008) 33–37.
[14] H.M. Ali, M. Raaif, Plasma oxidation of electron beam evaporated cadmium thin films, Thin Solid Films 520 (2012) 4418–4421.
[15] L.R. deLeon-Gutierrez, J.J. Cayente-Romero, J.M. Peza-Tapia, E. Barrera-Calva, J. C. Martínez-Flores, M. Ortega-Lopez, Some physical properties of Sn-doped CdO thin films prepared by chemical bath deposition, Mater. Lett. 60 (2006) 3866–3870.
[16] R. Kumaravel, K. Ramamurthi, V. Krishnakumar, Effect of indium doping in CdO thin films prepared by spray pyrolysis technique, J. Phys. Chem.Solids 71 (2010) 1545–1549.
[17] Y. Gulen, B. Sahin, F. Bayansal, H.A. Cetinkara, Solution-phase synthesis of un-doped, and Pb doped CdO films, Superlattice. Microst. 68 (2014) 48–55.
[18] J. Santos-Cruz, G. Torres-Delgado, R. Castanedo-Perez, S. Jimenez-Sandoval, O. Jimenez-Sandoval, C.I. Zuniga-Romero, J. Marquez Marın, O. Zelaya-Angel, Dependence of electrical and optical properties of sol–gel prepared undoped cadmium oxide thin films on annealing temperature, Thin Solid Films 493 (2005) 83–87.
[19] E. Pakizeh, Optical response, and structural properties of Fe-doped Pb (Zr 0.52 Ti 0.48) O3 nanopowders, J. Mater. Sci. 31 (2020) 4872–4881.
[20] F. Behzadi, E. Saievar-Iranizad, E. Pakizeh, Optical study on single-layer photoluminescent graphene oxide nanosheets through a simple and green hydrothermal method, J. Photochem. Photobiol., A 364 (2018) 595–601.
[21] A.M. Aboraia, A.A.A. Darwish, V. Polyakov, E. Erofeeva, V. Butova, Heba Y. Zahran, Alaa F. Abd El-Rehim, Hamed Algarni, I.S. Yahia, Alexander V. Soldatov, Structural characterization and optical properties of zeolitic imidazolate frameworks (ZIF-8) for solid-state electronics applications, Opt. Mater. 100 (2020) 109648.
[22] A.A.A. Darwish, A.M. Aboraia, Alexander V. Soldatov, I.S. Yahia, Deposition of Rhodamine B dye on flexible substrates for flexible organic electronic and optoelectronic: optical spectroscopy by Kramers-Kronig analysis, Opt. Mater. 95 (2019) 109219.
[23] M. Thambidurai, N. Muthukumarasamy, A. Ranjitha, Dhayalan Velauthapillai, Structural and optical properties of Ga-doped CdO nanocrystalline thin films, Superlattice. Microst. 86 (2015) 559–563.
[24] Bünyamin Şahin, Dual doping (Cu with rare-earth element Ce): An effective method to enhance the main physical properties of CdO films, Superlattice. Microst. 136 (2019) 106296.
[25] Elif Gürbüz, Raşit Aydin, Bünyamin Şahin, A study of the influences of transition metal (Mn, Ni) co-doping on the morphological, structural and optical properties of nanostructured CdO films, J. Mater. Sci. 29 (2018) 1823–1831.
[26] R. Aydin, B. Şahin, The role of Triton X-100 as a surfactant on the CdO nanostructures grown by the SILAR method, J. Alloys Compd. 705 (2017) 9–13.
[27] G. Vijayaprasath, R. Murugan, S. Asaithambi, P. Sakthivel, T. Mahalingam, Y. Hayakawa, G. Ravi, Structural and magnetic behavior of Ni/Mn co-doped ZnO nanoparticles prepared by co-precipitation method, Ceram. Int. 42 (2016) 2836–2845.
[28] P. Kumarn, P. Sharma, A.G. Joshi, R. Shrivastav, S. Dass, V.R. Satsangi, Nano porous hematite for solar hydrogen production, J. Electrochem. Soc. 159 (2012) 685–691.
[29] Harun Güney, Demet İskenderoğlu, the effect of Zn doping on CdO thin films grown by SILAR method at room temperature, Physica B 552 (2019) 119–123.
[30] S.G. Choi, L.M. Gedvilas, S.Y. Hwang, T.J. Kim, Y.D. Kim, J.Z. Perez, V.M. SanjoseTemperature-dependent optical properties of epitaxial CdO thin films determined by spectroscopic ellipsometry and Raman scattering, J. Appl. Phys. 113 (2013) 183515.
[31] P. Velusamy, R.R. Babu, K. Ramamurthi, E. Elangovan, J. Viegas, M.S. Dahlem, M. Arivanandhan, Characterization of spray pyrolytically deposited high mobility praseodymium doped CdO thin films, Ceram. Int. 42 (2016) 12675–12685.
[32] S.B. Jambure, C.D. Lokhande, Photoelectrochemical solar cells with chemically grown CdO rice grains on flexible stainless steel substrates, Mater. Lett. 106 (2013) 133–136.
[33] Harun Güney, The structural, morphological, optical, and electrical properties of Pb doped CdO thin films grown by spray method, Vacuum 159 (2019) 261–268.
[34] F.T. Thema, P. Beukes, A. Gurib-Fakim, M. Maaza, Green synthesis of Monteponite CdO nanoparticles by Agathosma betulina natural extract, J. Alloys Compd. 646 (2015) 1043–1048.
[35] DemetİskenderoğluHarunGüney, The effect of Zn doping on CdO thin films grown by SILAR method at room temperature, Phys. B Condens. Matter 552 (2019) 119–123.
[36] H. Bilz, D. Strauch, R.K. WehnerHandbook, Phys Licht und Materie Id, XXVlZd, Springer-Verlag, Berlin, 1984, p. 157.
[37] Z.V. Popovic, G. Stanisic, R. Kostic, Infrared and Raman spectra of CdO, Phys. Status Solidi(b) 165 (1991) K109.
[38] A. Ashrafi, K. Ostrikov, In encyclopedia of semiconductor nanotechnology, Appl. Phys. Lett. 98 (33119) (2011) 1–3.

[39] R. Cusco, J. Ibanez, N. Domenech-Amador, L. Artus, J. Zuniga-Perez, V. Munoz-Sanjosé, Raman scattering of cadmium oxide epilayers grown by metal-organic vapor phase epitaxy, J. Appl. Phys. 107 (63519) (2010) 1–4.
[40] A.A.M. Farag, A. Ashery, M.A. Salem, Electrical, dielectric characterizations and optoelectronic applications of epitaxially grown Co/n-CuO/p-Si heterojunctions, Superlattice. Microst. 135 (2019), 106277.
[41] G. Turgut, D. Tatar, Investigation of physical, electrical, and optical properties of sol-gel deposited Sc-loaded CdO films, Optik 145 (2017) 292–303.
[42] B. Hymavathi, B.R. Kumar, T.S. Rao, Investigations on physical properties of nanostructured Cr doped CdO thin films for optoelectronic applications, Procedia Mater. Sci. 10 (2015) 285–291.
[43] M. Benhalilib, C.E. Benouis, A. TiburcioSilver, F. Yakuphanoglu, A. Avila-Garcia, A. Tavira, R.R. Trujillo, Z. Mouffak, Luminescence and physical properties of copper doped CdO derived nanostructures, J. Lumin. 132 (2012) 2653–2658.
[44] F. Dagdelen, Z. Serbetci, R.K. Gupta, F. Yakuphanoglu, Preparation of nanostructured Bi-doped CdO thin films by a sol-gel spin coating method, Mater. Lett. 80 (2012) 127–130.
[45] Z. Sultan, N. Sultana, Analysis of reflectance and transmittance characteristics of optical thin film for various film materials, thicknesses, and substrates, J. Electr. Electron. Syst. 4 (2015), 1000160.
[46] K. Usharani, A.R. Balu, Properties of spray deposited Zn, Mg incorporated CdO thin films, J. Mater. Sci. Mater. Electron. 27 (2016) 2071–2078.
[47] G. Turguta, D. Tatar, Investigation of physical, electrical, and optical properties of sol-gel deposited Sc-loaded CdO films, Optik 145 (2017) 292–303.
[48] FerhundeAtaya Salih Kosea, VildanBilginb, IdrisAkyuz, In doped CdO films: Electrical, optical, structural, and surface properties, Int. J. Hydrogen Energy 34 (2009) 5260–5266.
[49] I.S. Yahia, G.F. Salem, M.S. Abd El-Sadek, F. Yakuphanoglu, Optical properties of Al-CdO nano-clusters thin films, Superlattice. Microst. 64 (2013) 178–184.
[50] Z.A. Alahmed, H.A. Albrithen, A.A. Al-Ghamdi, F. Yakuphanoglu, Optical band gap controlling of nanostructure Mn-doped CdO thin films prepared by a sol-gel spin coating method, Optik 126 (2015) 575–577.
[51] F. Dagdelen, Z. Serbetci, R.K. Gupta, F. Yakuphanoglu, Preparation of nanostructured Bi-doped CdO thin films by a sol-gel spin coating method, Mater. Lett. 80 (2012) 127–130.
[52] I.S. Yahia, G.F. Salem, J. Iqbal, F. Yakuphanoglu, Linear and nonlinear optical discussions of nanostructured Zn-doped CdO thin films, Phys. B Condens. Matter 511 (2017) 54–60.
[53] I.S. Yahia, G.F. Salem, M.S. Abd El-Sadek, F. Yakuphanoglu, Optical properties of Al-CdO nano-clusters thin films, Superlattice. Microst. 64 (2013) 78–184.
[54] Y. Zhu, R.J. Mendelsberg, J. Zhu, J. Han, A. Anders, Dopant-induced band filling and bandgap renormalization in CdO : In films, J. Phys. D Appl. Phys. 46 (2013), 195102.
[55] M.V. Kumar, S. Muthulakshmi, A.A. Paulfrit, J. Pandiarajan, N. Jeyakumaran, N. Prithivikumaran, Structural and optical behaviour of thermally evaporated p-type nickel oxide thin film for solar cell applications, Int. J. Chem. Res. 6 (13) (2014) 5174–5177.
[56] Kenji Kamide, Toshiaki Dobashi, Chapter 7, Light Scattering, Physical Chemistry of Polymer Solutions, Elsevier B.V., 2000, pp. 377–442.
[57] Nadia A.A. Elkanzi, A.A.M. Farag, N. Roushdy, A.M. Mansour, Design, fabrication, and optical characterizations of pyrimidine fused quinolone carboxylate moiety for photodiode applications, Optik 216 (2020) 164882.
[58] S.H. Wemple, M. DiDomenico, Behavior of the electronic dielectric constant in covalent and ionic materials, Phys. Rev. B 3 (1971) 1338–1351.
[59] N.M. Ravindra, Preethi Ganapathy, Jinsoo Choi, Energy gap–refractive index relations in semiconductors – An overview, Infrared Phys. Technol. 50 (2007) 21–29.
[60] K. Tanaka, Optical properties and photoinduced changes in amorphous AsxS100-x films, Thin Solid Films 66 (1980) 271–279.
[61] A.S. Hassanien, Studies on dielectric properties, optoelectrical parameters, and electronic polarizability of thermally evaporated amorphous Cd50S50-xSex thin films, J. Alloys Compd. 671 (2016) 566–578.
[62] R.P.S.M. Lobo, The Optical Conductivity of High-Temperature Superconductors, High-Temperature Superconduct, 2011, pp. 103–146.
[63] A.A.M. Farag, I.S. Yahia, M.S. Al-Kotb, Nanostructure, and enhancement of the optical properties of Tb-doped NiO for photodiode applications, Chin. J. Phys. 64 (2020) 87–102.
[64] I.S. Yahia, G.F. Salem, Javed Iqbal, F. Yakuphanoglu, Linear and nonlinear optical discussions of nanostructured Zn-doped CdO thin films, Physica B 511 (2017) 54–60.
[65] H. Ticha, L. Tichy, Semiempirical relation between non-linear susceptibility (refractive index), linear refractive index and optical gap, and its application to amorphous chalcogenides, J. Optoelectron. Adv. Mater. 4 (2002) 381–386.
[66] V. Ganesh, Mohd Shkir, S. AlFaify, I.S. Yahia, H.Y. Zahran, A.F. AbdEl-Rehim, Study on structural, linear, and nonlinear optical properties of spin-coated N doped CdO thin films for optoelectronic applications, J. Mol. Struct. 1150 (2017) 523–530.
[67] A.F. Qasrawi, Ansam M. Alsabe, ZnSe/Al/ZnSe nanosandwiched structures as dual Terahertz–Gigahertz signal receivers, Mater. Res. Express 6 (2019) 65704.
[68] R. Wang, J. Zhuge, R. Huang, Y. Tian, H. Xiao, L. Zhang, Ch Li, X. Zhang, Y. Wang, IEEE Trans. Electron. Dev. 54 (2007) 1288–1294.
[69] Seham Reef Alharbi, A.F. Qasrawi, Effects of Au nanoslabs on the performance of CdO thin films designed for optoelectronic applications, Physica E 125 (2021), 114386.